

# Electrochemical synthesis of copper (II) based metal organic frameworks: Determination of structure by Single X-ray diffraction crystallography and other supportive techniques

Kalawati Saini<sup>1</sup>, Florence Jojeph<sup>2</sup> and Smriti S. Bhatia<sup>3</sup>

<sup>1,3</sup> *Miranda House, Chemistry Department, University of Delhi, Patel Chest Marg, New Delhi 110007, India*

<sup>2</sup> *The Shri Ram School, Chemistry Department, Gurgaon 122002, India*

\*Corresponding author

DOI: 10.5185/amp.2018/7002

www.vbripress.com/amp

## Abstract

The copper (II) extended metal organic frameworks with oxalic acid (ox = oxalate)  $[Na_2(Cu(ox)_2) \cdot H_2O]$  and  $[(NH_4)_2\{Cu(ox)_2(H_2O)_2\}\{Cu(ox)_2\}] \cdot H_2O$  have been synthesized using electrochemical route at room temperature and applied potential at 12.5 V. Herein copper rod has taken as a working electrode and platinum wire as a reference electrode. The single crystal X-ray diffraction (SXRD) and other supportive techniques like as PXRD, TGA/DTA, FT-IR have been used for structural characterizations. Metal organic frameworks (MOFs) are crystalline in nature where the ligands and metal ions are assembled infinitely resulting in one, two or three-dimensional networks having direct metal-ligand coordination. The growth of the solids has been explained corresponding to the mechanistic approach proposed by Ramanan and Whittingham. The crystal packing has been influenced by the supporting electrolyte. The electrolytic method is a simple process, low energy consumption, high yield, easy control and no environmental pollution. Copyright © 2018 VBRI Press.

**Keywords:** Working electrode, platinum electrode, crystal packing, MOFs, single crystal.

## Introduction

Metal-organic frameworks play an important role in hydrogen storage problem associated with hydrogen-fueled vehicles [1]. David J. Collins and Hong-Cai Zhou have studied hydrogen storage in metal-organic frameworks [2]. Sudeshna Bhattacharya has designed the chiral Co (II)-MOFs and studied their application in environmental remediation and waste water treatment [3]. The solvo-thermal method has been used for preparing the Co-MOFs. These synthesized Co-MOFs have been used for the photocatalytic hydrogen evolution. The copper metal organic frameworks have been investigated for their potential applications such as catalysis, electrical conductivity, luminescence and magnetism. Copper oxalate and malonate complexes have been researched for their application in molecular magnetic devices. Structural correlation with magnetic and photocatalytic activity has been studied for hexanuclear copper-based secondary building unit [4]. Pravas Deria has synthesized Zirconium-based metal-organic frameworks which are ultra-porous and very stable. He also studied their fitw Topology [5]. The electrical properties have been determined by Keith T. Butler et al [6]. Some MOFs with porous structure and large surface area have been investigated for gas storage and catalysis [7-9]. These materials have unique combination of optical and electronic properties. Because of this these materials have been used into

photocatalytic, photovoltaic, and electrochemical devices [10-18]. The MOFs of Ag[I] having  $\pi$ -stacked have been reported in the literature for very high electrical conductivity [19].

B.F. Hoskins and R. Robson et al have investigated the porous coordination polymer which shows an anion exchange properties [20]. The 2D  $[Cd^{II}(4,4'-bpy)_2]$  (bpy = bipyridine) coordination polymer have been reported by Fujita et al [21]. Which shows excellent catalytic properties. The research group of Yaghi has studied the adsorption of guest molecules in 1995 [22]. Moore and Kitagawa's group have reported the gas adsorption at ambient temperature [23-24].

The crystal structure and magnetic properties of 1D chains of Cu (II) with oxalate as one of the bridging ligands have been reported in the literature. The crystal engineering of many functional supramolecular materials have been designed on the basis of coordination force, hydrogen bonding and other intermolecular interactions [25-30]. Though there are still many challenges to understand the mechanism of these tailor-made molecular materials. Because the structural control in making such type materials has been done by the weak interactions [31]. The crystal engineering has been further investigated when the starting reactants comprise two or more distinct molecular / ionic component. The hybrid nature of the resultant materials is responsible for their potential

applications. The formation of the molecular assembly into the prescribed crystalline architecture via hydrogen bonding is attracting the attention of researchers since two decades [32-33]. There is reported in the literature that charge-assisted hydrogen bonds are strong, directional as well as compliant in nature. In this context the research paper reported by Ramanan and Whittingham in 2006 is very significant in which they have shown the several neutral MOFs [34].

The nature of the ligand play very important for producing the flexibility, functionality and chirality in the MOFs. Weaker interactions, such as hydrogen bonding or  $\pi$ - $\pi$  stacking are important for the packing of all type of structure like as 1D chains, 2D sheets and 3D frameworks [35]. The ligands which are used in the formation of coordination polymers have to bridge between metal oxides or metal ions. The multidentate ligands with two or more donor atoms are used for getting such type of coordination polymers. The diversity of organic ligands play important role for the different structural topologies. The physical properties can be tuned by selecting the organic ligand very carefully. The selection of a particular ligand affect the various properties such as catalysis, electrical conductivity, luminescence, magnetism, non-linear optics or zeolitic behavior [36-40]. The MOFs of Copper with dicarboxylic acid have been synthesized by G.R. Deshraj, G.R and M. Nishio [41-42]. The copper-azido coordination polymer,  $[\text{Cu}_2(\text{N}_3)_3(\text{L})]_n$  ( $\text{L}$ =pyrazine-2-carboxylic acid) having unique characteristic has been prepared by hydrothermal method in the aqueous medium [43]. The hexanuclear copper-based secondary building units are responsible for the photocatalytic activity and magnetic properties [44].

The goal of this paper is to synthesize single phase MOFs of copper with oxalate and understand their formation in terms of the reacting molecular precursors by electrochemical route without using copper salt. Herein copper electrode works as the source of  $\text{Cu}^{+2}$  ions. Because as the potential is applied, oxidation of Cu from copper rod (electrode) in to  $\text{Cu}^{+2}$  takes place in the electrochemical cell. The morphology of the product (powder or single crystals) can be changed with variation in experimental parameters such as pH, applied external potential, concentration of ligand, type of supportive electrolyte, temperature and scan rate (mV/s). The structural characterizations have been done by using different techniques like as FTIR, TGA, single crystal X-ray diffraction (SXRD) and powder x-ray diffraction (PXRD) respectively. The MOFs of KS1 can be use as a magnetic materials.

One of the main advantages of electrochemical synthesis at room temperature is that weak interactions (hydrogen bonds,  $\text{CH}\dots\pi$ ,  $\pi\dots\pi$  interactions etc.) are retained at room temperature. It means they are not broken at room temperature. This provides a new way of synthesis of MOFs. The presence of weak interactions in the synthesized MOFs are responsible various structural topologies and functionalities. So the

electrochemical method is very important tool in preparing of new MOFs at room temperature.

## Experimental

### Materials/chemicals details

All chemicals have been procured commercially and used directly without purification. Oxalic acid and sodium hydroxide of A.R. grade purchased from Merck Limited, India. Copper metal rod (99.9% pure, metal basis) has been obtained from Alfa Aesar. The Pt wire (99.9% pure, metal basis) was purchased from SINSIL International Pvt. Ltd. Which has been used as a reference electrode for the synthesis of copper based MOFs.

All the solutions have been prepared in double de-ionized water. The 20 ml solution of 0.1 M oxalic acid has been taken for both set up. In the set -1 the amount of NaOH (3.145mM) has been dissolved where as in the set-2 one mL (1mL) of liquor ammonia has been added as a supporting electrolyte.

### Material synthesis / reactions

#### $[\text{Na}_2\text{Cu}(\text{ox})_2]\cdot\text{H}_2\text{O}$ , KS1

The oxalic acid (0.2521 g, 0.1M) has been dissolved in 20 ml of water. In this solution the amount of sodium hydroxide corresponding to (3.145mM) has been added. Copper electrode has been taken as the anode and Pt wire has been taken as the counter electrode. External potential (12.5 V) has been applied for 12 hours at room temperature for this set-up. Blue colored solution has been obtained. Blue needle-like crystals of  $[\text{Na}_2\text{Cu}(\text{ox})_2(\text{H}_2\text{O})]$  have been obtained by slow evaporation of the resulting blue colored solution at room temperature after fifteen days. Potential (12.5V) has been applied for a fixed time interval using a potentiostat (Potentiostat Wenking Model POS 73) and simple potential applier.

#### $[(\text{NH}_4)_2\{\text{Cu}(\text{ox})_2(\text{H}_2\text{O})\}_2\{\text{Cu}(\text{ox})_2\}]\cdot\text{H}_2\text{O}$ , KS2

Blue block-type crystals of  $[(\text{NH}_4)_2\{\text{Cu}(\text{ox})_2(\text{H}_2\text{O})\}_2\{\text{Cu}(\text{ox})_2\}]\cdot\text{H}_2\text{O}$  have been obtained by using above-mentioned method. The compound KS2 has been prepared by adding 1mL of ammonia solution. The crystal of this metal organic framework has also obtained by slow evaporation of set -2 reaction solution after applying same potential as given for set-1. Herein simple potential applier has been used for synthesis of this compound.

### Characterizations/device fabrications/response measurements

#### Powder X-ray diffraction

Powder X-ray powder diffraction data have been collected with a Bruker D8 Advance diffractometer using Ni-filtered  $\text{Cu-K}\alpha$  radiation. Data have been collected with a step size of  $0.05^\circ/\text{s}$ . The scan range ( $2\theta$ ) has been kept from  $2^\circ$  to  $60^\circ$ .

### Single Crystal X-ray Diffraction

Single-crystal X-ray diffraction has been carried out by using a Bruker AXS SMART Apex D8 CCD diffractometer equipped with a fine-focus sealed-tube X-ray source (MoK $\alpha$  radiation,  $\lambda = 0.71073$  Å, graphite monochromator) operating at 50 kV and 45 mA. Crystals of KS1 and KS2, have been mounted on glass fibers at room temperature. Frames were collected with 0.38 intervals in  $\theta$  and  $\omega$  for 30 s per frame, in such a way that a hemisphere of data has been collected. Raw data collection and cell refinement been obtained by using SMART; data reduction has been done by using SAINT+ and corrected for Lorentz and polarization effects [45]. Absorption corrections have been done by using the SADABS routine. Structures have been solved by direct methods by using SHELXTL and refined by full-matrix least-squares on  $F^2$  by using SHELX-9 [46]. Non-hydrogen atoms have been refined with anisotropic displacement parameters during the final cycles. Hydrogen atoms have been placed in calculated positions with isotropic displacement parameters set to 1.20U $_{eq}$  of the attached atom.

### Thermal analysis

The Perkin–Elmer TGA7 model has been used for TG analysis. This analysis has been carried out in presence of inert medium (N $_2$  atmosphere) with a heating rate of 10°C/min. This analysis has been done for testing the thermal stability of the obtained products and to ascertain the temperature at which decomposition of the compound take place.

### Vibrational spectroscopy

Nicolet 5DX spectrophotometer with pressed KBr pellet has been used for taking Fourier Transformed Infra Red (FTIR) spectra. The range of spectrum has been fixed from 4000 to 400cm $^{-1}$ .

### Results and discussion

The electrochemical technique represents one of the simplest and most direct method for carrying out oxidation or reduction reactions. The removal or addition of electrons happen without the addition of external agents. The synthesis involves the oxidation or reduction of solute species at inert electrodes to yield direct products. But sometimes we get the intermediate species, which subsequently decomposes and gives the products. For example if potential is applied between copper and platinum electrode, copper gets oxidized and cupric ions enter in to the reaction medium. Therefore if the reaction medium contains ligands capable of chelating with copper, the crystal of MOF can be formed either at the electrode surface or by the slow evaporation of the reaction solution.

In our experiments the copper electrode is taken as anode it oxidizes to give cupric ions in solution. These ions may undergo further hydrolysis to form soluble molecular precursors as shown in the following scheme, **Fig. 1**. When we increase reaction time, the color of the

solution changes from colorless to intense blue colour which shows the complex formation of copper ions with ligands.

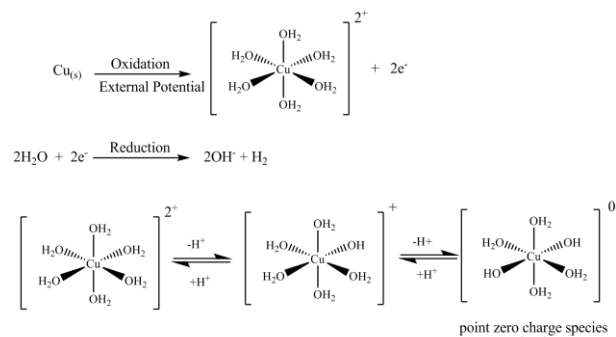


**Fig 1.** Scheme showing the results obtained using the electrochemical route.

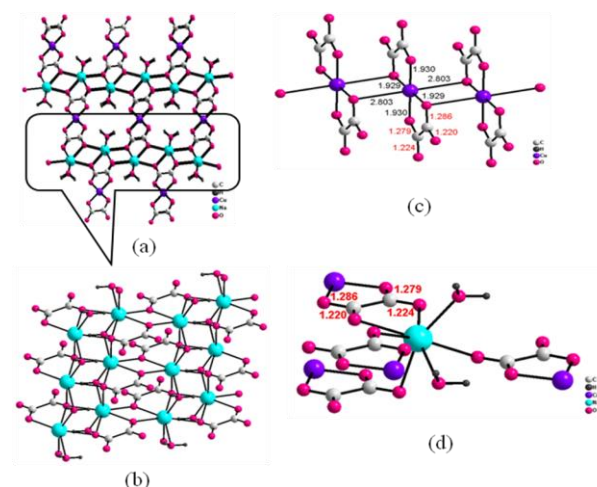


**Fig. 2.** Three-Dimensional sodium copper oxalate framework in **KS1** (a). The sodium oxalate sheets linked to copper oxalate chains result in the 3D framework. (b), One-Dimensional copper oxalate chains (c), Hepta-coordinated sodium center showing interactions between the oxalate and sodium centers (d).

### Crystal structure of [Na $_2$ Cu(ox) $_2$ ].H $_2$ O

In **KS1**, copper exhibits octahedral geometry where it coordinates to two oxalate groups on its equatorial plane and coordinated oxygen of the neighboring copper center on its axial plane forming one-dimensional chains as shown in **Fig. 2** (c). The fifth and sixth coordination is satisfied along Cu-O (2.803 Å) bond resulting from John Teller distortion. The bond distances between the carbons and oxygen suggested that hydroxyl oxygen coordinates with the copper centre rather than the carbonyl oxygen. The carbonyl's oxygen are further linked to sodium centers which subsequently gives a three-dimensional metal organic frameworks. This is shown in **Fig.2** (a, b). Each sodium center is hepta-coordinated. It coordinates to two water molecules, both the carbonyl groups of the same oxalate moiety and three other carbonyl's oxygen of neighboring oxalate moiety as shown in **Fig. 2** (d). We have made an attempt to understand the formation of the solid based on Raman and Whittingham's hypothesis as shown in **Fig. 3**. The crystallographic

data of **KS1** have been given in **Table 1**. The structure of **KS1** matches to the reported structure in literature but herein it has been synthesized via electrochemical route [47].

**Table 1.** The crystallographic details of compound  $[\text{Na}_2\text{Cu}(\text{ox})_2]\cdot\text{H}_2\text{O}$ , **KS1**

Crystal system	Triclinic
Space group	P-1
Molecular Weight(g)	321.6
<i>a</i> (Å)	7.536(3)
<i>b</i> (Å)	9.473(4)
<i>c</i> (Å)	3.576(2)
$\alpha$ (°)	81.90(6)
$\beta$ (°)	103.77(5)
$\gamma$ (°)	108.09(4)
<i>V</i> (Å <sup>3</sup> )	235.07(408)
<i>Z</i>	1

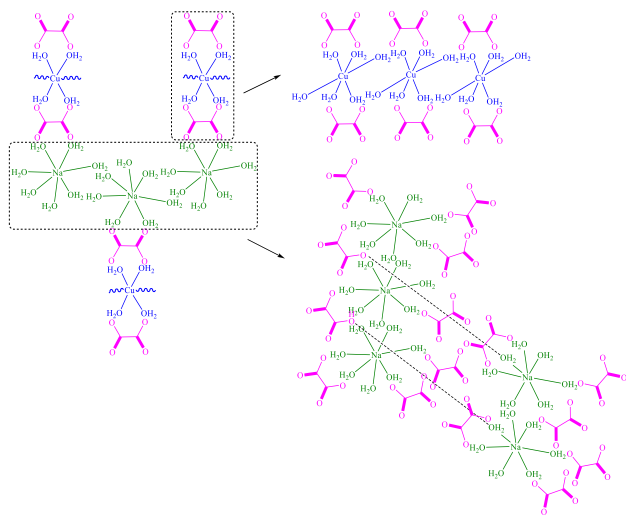


**Fig. 3.** Soluble cupric ions condense with oxalate ions to form 1D chains, which are further linked by hepta coordinated sodium centers. The bold lines indicate double bond. In the presence of NaOH the oxalic acid gets ionized therefore self-assembly takes place between ion pairs.

The phase purity of the above solid has been carried out by using PXRD. The simulated pattern matches well with the PXRD pattern obtained with the bulk material. The indexed PXRD pattern of **KS1** has been given in **Fig. S1** (see supporting information).

The FTIR spectra (see supporting information, **Fig. S2**) of MOF of **KS1** shows characteristic bands of  $\nu(\text{Cu-O})$ ,  $\nu(\text{C-O})$ ,  $\nu(\text{ring})$ ,  $\nu(\text{COO}^-)$ ,  $\nu(\text{C-H})$ ,  $\nu(\text{O-H})$  and  $\text{H}_2\text{O}$ . The corresponding vibrational peaks have been assigned at  $904.00\text{-}777.68\text{cm}^{-1}$ ,  $1324.78\text{-}1116.66\text{cm}^{-1}$ ,  $1411.45\text{cm}^{-1}$ ,  $1324.78\text{-}1116.66\text{cm}^{-1}$ ,  $1411.45\text{cm}^{-1}$ ,  $1651.06\text{cm}^{-1}$ ,  $2541.06\text{cm}^{-1}$ ,  $2929.18\text{-}2766.39\text{cm}^{-1}$ ,  $3446.92\text{cm}^{-1}$  and  $3532.49\text{cm}^{-1}$ . There has been found to be some displacement in the characteristic vibrational peaks which attributes the formation of complex of Cu(II) with oxalate.

Thermal dissociation of the **KS1** compound has been done from  $50\text{-}900^\circ\text{C}$ . The heat rate has been kept

$10^\circ\text{C}/\text{min}$ . The TGA has been given in supportive information (**Fig. S3**).

The crystalline water molecule come from the MOFs in the range  $110\text{-}200^\circ\text{C}$  in a single step. Which is generally called dehydration process. The second ( $220\text{-}280^\circ\text{C}$ ) third ( $280\text{-}480^\circ\text{C}$ ) steps are corresponds to the pyrolysis of the ligand (first coordinated water then oxalate) and the fourth step  $480\text{-}650^\circ\text{C}$  corresponds to the forming  $\text{CuO}$  and  $\text{Na}_2\text{CO}_3$ . All steps of TGA support the formation of MOFs of copper with oxalate.

### Crystal Structure of $[(\text{NH}_4)_2\{(\text{Cu}(\text{ox})_2(\text{H}_2\text{O})_2)\{\text{Cu}(\text{ox})_2\}]\cdot\text{H}_2\text{O}$ , **KS2**

The two copper atoms in unit cell occupy special positions and situated to each other at a distance of  $5.313\text{Å}$ .  $\text{Cu}1$  is coordinated with four oxalate oxygen atoms at a distance of  $\approx 2\text{Å}$  at the corners of square (equatorial position). The two water oxygen at a distance  $2.449\text{Å}$  are lied on a line approximately perpendicular and thus complete the distorted octahedral configuration around  $\text{Cu}1$ . The second cupric ion  $\text{Cu}2$  also has a planar environment of four coordinated oxalate oxygen however, it does not coordinate with remaining water molecule. The octahedral coordination is completed by oxygen ( $2.659\text{Å}$ ) belonging to oxalate 1. This distance is found to be less than the reported in the literature [48]. In this MOF the C-C bonds in both the two nonequivalent oxalate ions in the unit cell are single bonds ( $1.548\text{Å}$  and  $1.556\text{Å}$ ). These bond length are corresponding with the results of Jeffrey and Parry. Where the carboxyl groups of the oxalate ion are separated by a pure  $\sigma$  bond. It means there is no  $\pi$  conjugation across the molecule [49]. Both the oxalate ions are slightly non-planar. The environment of the  $\text{NH}_4^+$  ions consists of eight nearest oxygen atoms at a distance  $2.968\text{Å}$  and  $3.149\text{Å}$ . Out of these four atoms are at corners of distorted tetrahedron and perhaps take part in the formation of  $\text{N-H}\cdots\text{O}$  bond. The non-equivalent oxalate within the unit cell are held together by  $\text{O-H}\cdots\text{O}$  bond from water molecule and three dimensional structure is built by linking these aggregates to their centro symmetrically related units in the neighbouring cell by alternate  $\text{Cu-O}$  and  $\text{NH}_4^+ \text{-O}$  interactions. Thus the hydrogen bondings results the 3D structure.

Out of two  $\text{NH}_4^+$  ions one is presented from  $\text{Cu}1$  at a distance  $3.726\text{Å}$  and another one at  $8.107\text{Å}$  respectively. And from  $\text{Cu}2$  at a distance  $4.439\text{Å}$  and  $5.175\text{Å}$  respectively. The experimental values of bond angles and bond lengths have been given in a **Table S3** which has been given in supportive information. The chain structure of MOF of **KS2** along a-axis has been shown in **Fig. 4**. In this structure the bond distances are found to be as follows  $\text{N1-O1W} = 3.042\text{Å}$ ,  $\text{N2-O2W} = 3.193\text{Å}$ ,  $\text{N1-N1} = 5.467\text{Å}$ ,  $\text{N2-N2} = 4.147\text{Å}$ ,  $\text{N1-N1} = 3.849\text{Å}$ ,  $\text{N2-N2} = 3.810\text{Å}$ ,  $\text{N2-N1} = 4.999\text{Å}$ ,  $\text{N2-N1} = 4.185\text{Å}$ . The 2D structure have been given in **Fig. 5** and **Fig. 6**. When we open crystal information file (cif) in mercury (Hg) software, crystal structures

have been shown in **Figs S4, S5, S6**. **Fig. S4** shows extended crystal structure through oxygen atoms of carboxyl group. **Fig. S5** shows atomic lengths. **Fig S6** shows packing of crystal structure. The structure refinement parameters and crystal data for compound KS2 have been given in **Table 2**.

The FTIR spectra (**Fig. S7**) of MOF of **KS1** shows characteristic bands of  $\nu(\text{Cu-O})$ ,  $\nu(\text{C-O})$ ,  $\nu(\text{ring})$ ,  $\nu(\text{COO}^-)$ ,  $\nu(\text{C-H})$ ,  $\nu(\text{NH}_4^+)$  and  $\text{H}_2\text{O}$ . The corresponding vibrational peaks have been assigned at  $885.80\text{ cm}^{-1}$ ,  $1300.85\text{--}1184.22\text{ cm}^{-1}$ ,  $1436.73\text{ cm}^{-1}$ ,  $1300.85\text{--}1184.22\text{ cm}^{-1}$ ,  $1622.83\text{ cm}^{-1}$ ,  $2366.70\text{ cm}^{-1}$ ,  $2933.60\text{ cm}^{-1}$ ,  $3376.72\text{ cm}^{-1}$  and  $3583.49\text{ cm}^{-1}$ . These values has been given in **Table S2** in the supportive information. There has also been found to be some displacement in the characteristic vibrational peaks which attributes the formation of  $\text{Cu(II)}$  with oxalate.

**Table 2.** Crystal data and structure refinement parameters for compound KS2.

Chemical formula	C H Cu N O
sum	
chemical formula weight	299.61
Crystal system ,space group	Triclinic , P-1
Unit Cell dimension	
a(Å)	6.943(2)
b(Å)	8.909(3)
c(Å)	9.036(3)
$\alpha$ (°)	107.566(5)
$\beta$ (°)	97.753(6)
$\gamma$ (°)	96.599(6)
cell volume (Å <sup>3</sup> )	520.8(3)
cell formula units Z	7
cell measurement temperature	273(2)
cell measurement reflns used	3801
cell measurement theta min(°)	2.40
cell measurement theta max (°)	28.36
diffn ambient temperature (K)	273(2)
diffn radiation wavelength(Å)	0.71073
diffn radiation type	MoK $\alpha$
diffn radiation source	'fine-focus sealed tube'
diffn radiation monochromator	graphite
diffn measurement device type	CCD area detector
diffn measurement method	phi and omega scans
reflns number total	2506
computing cell refinement	Bruker SMART
computing data reduction	Bruker SAINT
computing structure solution	SHELXS-97(Sheldrick, 1990)
computing structure refinement	SHELXL-97(Sheldrick, 1997)
computing molecular graphics	Bruker SHELXTL
refine ls R factor all	0.0399
refine ls R factor gt	0.0372
refine ls WR factor ref	0.1167
refine ls WR factor gt	0.1146
refine ls goodness of fit ref(GOF)	1.226
refine ls shift/su max	1.234
refine ls shift/su mean	0.012

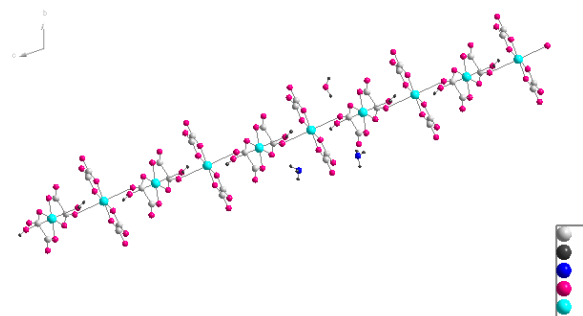


**Fig. 4.** Chain Structure of  $[(\text{NH}_4)_2\{(\text{Cu}(\text{ox})_2(\text{H}_2\text{O})_2)\{\text{Cu}(\text{ox})_2\}\}.\text{H}_2\text{O}$ , KS2\_ along a axis.

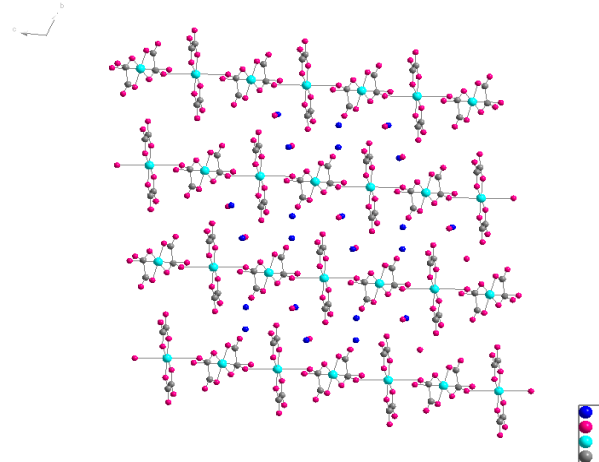


**Fig. 5.** 2D Structure of  $[(\text{NH}_4)_2\{(\text{Cu}(\text{ox})_2(\text{H}_2\text{O})_2)\{\text{Cu}(\text{ox})_2\}\}.\text{H}_2\text{O}$ , KS2\_ along a axis.

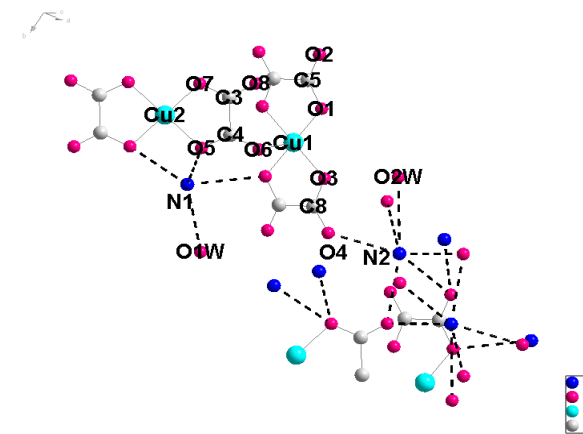


**Fig. 6.** Building of 3D structure of  $[(\text{NH}_4)_2\{(\text{Cu}(\text{ox})_2(\text{H}_2\text{O})_2)\{\text{Cu}(\text{ox})_2\}\}.\text{H}_2\text{O}$

## Conclusion

The bidentate oxalic acid ligand forms a 3D framework of copper, in presence of the sodium hydroxide when it is used as supporting electrolyte and in presence of ammonia solution it gives 2D frameworks which further produces 3D structure through weak interactions (H-bonding). The fifth and sixth coordination is satisfied along  $\text{Cu-O}$  ( $2.803\text{ \AA}$ ) bond resulting from John Teller distortion in MOF of **KS 1**. The bond distances between the carbons and oxygen suggested that hydroxyl oxygen coordinates with the copper centre rather than the carbonyl oxygen. Surface interactions play an important role in growth of solids.



We have observed that with the increase in external potential, the rate of oxidation of metal increases. The rate of complexation also increases with the formation of powder precipitate. But at an optimum applied potential, controlled oxidation of metal electrode take place which subsequently forms the soluble metal – ligand complex. After fifteen days, the fine blocks type crystals of the complex are obtained on slow evaporation at room temperature. We have presented the explanation for the different morphology on the basis of the proposed pathway of structural organization by Raman and Whittingham. The solvated metal ions form the starting point for solid formation. Subsequently the ligand molecules attach themselves to the central metal ion, forming a template for crystal growth. Dehydration on slow evaporation leads to the formation of the solid.

Thus the electrolytic method follow the principle of green chemistry in which we get high yield and no by-products. Since herein we have kept all set-up at room temperature and applied very low potential. So this approach of synthesis consume very less energy and no pollution. By understanding the role of anode, ligand, applied external potential and content and concentration of reaction mixture in solid organization, we believe that the electrochemical route for MOF synthesis holds lot of promises for future explorations. The synthesized MOF [Na<sub>2</sub>Cu(ox)<sub>2</sub>(H<sub>2</sub>O)] can be used as a molecular magnet.

#### Acknowledgements

Authors thank to Professor A. Ramanan, Chemistry Department, Indian Institute of Technology Delhi for his valuable guidance for this work and also thank to Indian Institute of Technology for providing facility for SXRD, PXRD, TGA and FTIR analysis. The Author also thank to CSIR (File No. 09/086(0830)/2007-EMR-I) for providing fund for this work.

#### Supporting information

Supporting informations are available from VBRI Press.

#### References

- MacGillivray, L. R. (Eds.); *Metal-Organic Frameworks: Design and Application*; John Wiley & Sons: Hoboken, New Jersey, USA, **2010**.
- Collins, D. J.; Hong-Cai Zhou, H.C.; *J. Mater. Chem.*, **2007**, *17*, 3154.
- Bhattacharya, S.; Bala, S.; Mondal, R.; *RSC Adv.*, **2016**, *6*(30), 25149.
- Sukhen Bala, S.; Indranil Mondal, I.; Goswami, A.; Ujjwal Pal, U.; Mondal, R.; *J. Mater. Chem. A*, **2015**, *3*(40), 20288.
- Bala, S.; Bhattacharya, S.; Goswami, A.; Adhikary, A.; S. Konar, S.; Mondal, R.; *Cryst. Growth Des.*, **2014**, *14* (12), 6391.
- Butler, K. T.; Hendon, C.; Walsh, A.; *J. Am. Chem. Soc.*, **2014**, *136*, 2703.
- Furukawa, H.; Cordova, K. E.; O'Keeffe, M.; Yaghi, O. M.; *Science*, **2013**, *341*, 1230444.
- Furukawa, H.; Ko, N.; Go, Y. B.; Aratani, N.; Choi, S. B.; Choi, E.; Yazaydin, A. O.; Snurr, R. Q.; O'Keeffe, M.; Kim, J.; Yaghi, O. M.; *Science*, **2010**, *329*, 424.
- Peng, Y.; Krungleviciute, V.; Eryazici, I.; Hupp, J. T.; Farha, O. K.; Yildirim, T.; *J. Am. Chem. Soc.*, **2013**, *135*, 11887.
- Brozek, C.; Dincă, M.; *J. Am. Chem. Soc.*, **2013**, *135*, 12886.
- Alvaro, M.; Carbonell, E.; Ferrer, B.; Llabrés i Xamena, F. X.; García, H.; *Chem. Eur. J.*, **2007**, *13*, 5106.
- Nijem, N.; Wu, H.; Canepa, P.; Marti, A.; Balkus, K. J.; Thonhauser, T.; Li, J.; Chabal, Y. J.; *J. Am. Chem. Soc.*, **2012**, *134*, 15201.
- Hendon, C. H.; Tiana, D.; Walsh, A.; *Phys. Chem. Chem. Phys.*, **2012**, *14*, 13120.
- Dhakshinamoorthy, A.; Alvaro, M.; Garcia, H.; *Chem. Commun.*, **2012**, *48*, 11275.
- Zhan, W. W.; Kuang, Q.; Zhou, J.-Z.; Kong, X.-J.; Xie, Z.-X.; Zheng, L.-S.; *J. Am. Chem. Soc.*, **2013**, *135*, 1926.
- Llabrés i Xamena, F. X.; Corma, A.; Garcia, H.; *J. Phys. Chem. C*, **2007**, *111*, 80.
- Horiuchi, Y.; Toyao, T.; Saito, M.; Mochizuki, K.; Iwata, M.; Higashimura, H.; Anpo, M.; Matsuoka, M.; *J. Phys. Chem. C*, **2012**, *116*, 20848.
- Davydovskaya, P.; Pohle, R.; Tawil, A.; Fleischer, M.; *Sensor. Actuat. B Chem.*, **2013**, *187*, 142.
- Hutchins, K. M.; Rupasinghe, T. P.; Ditzler, L. R.; Swenson, D. C.; Sander, J.R.; Baltrusaitis, J.; Tivanski, A. V.; MacGillivray, L. R.; *J. Am. Chem. Soc.*, **2014**, *136*(19), 6778.
- Hoskins, B. F.; Robson, R.; *J. Am. Chem. Soc.*, **1990**, *112*, 1546.
- Fujita M.; Kwon, Y. J.; Washizu, S.; Ogura, K.; *J. Am. Chem. Soc.*, **1994**, *116*, 1151.
- Yaghi, O. M.; Li, G.; Li, H.; *Nature*, **1995**, *378*, 703.
- Gardner, D. G. B.; Lee, S.; Moore, J. S.; *J. Am. Chem. Soc.*, **1995**, *117*, 11600.
- Kondo, M.; Yoshitomi, T.; Seki, K.; Matsuzaka, H.; Kitagawa, S.; *Angew. Chem.*, **1997**, *109*, 1844. *Angew. Chem.*, Int. Ed. Engl. **1997**, *36*, 1725.
- Schmidt, G. M. J.; *J. Pure Appl. Chem.*, **1971**, *27*, 647 (b) Deshraj, G. R. *Crystal Engineering: The Design of Organic Solids*; Elsevier: Amsterdam, **1989**.
- Janiak, C.; *Dalton Trans.*, **2003**, *14*, 2781.
- Nishio, M.; *Cryst. Eng. Comm.*, **2004**, *6*, 130.
- Desiraju, G. R.; *J. Mol. Struct.*, **2003**, *656*, 5.
- Moulton, B.; Zaworotko, M. *J. Chem. Rev.*, **2001**, *101*, 1629.
- (a) Steiner, T. *Angew. Chem.*, Int. (Ed.), **2002**, *41*, 48. (b) Jeffrey, G.A.; Saenger, W. *Hydrogen Bonding in Biological Structure*; Springer: Berlin, **1991**.
- Holman, K. T.; Pivovarov, A.M.; Swift, J.A.; Ward, M.D.; *Acc. Chem. Res.*, **2001**, *34*, 107.
- (a) Beatty, A.M.; *Coord. Chem. Rev.* **2003**, *246*, 131 (b) Sharma, C.V.K.; *Cryst. Growth Des.*, **2002**, *2*, 465. (c) Aakeroy, C. B.; Salmon, D. J.; *Cryst. Eng. Comm.*, **2005**, *7*, 439.
- Ward, M. D.; *Chem. Commun.*, **2005**, *47*, 5838.
- Ramanan, A.; Whittingham, M. S.; *Cryst. Growth Des.*, **2006**, *6*, 2419.
- Hutchins, K. M.; Rupasinghe, T.P.; Ditzler, L.R.; Swenson, D. C.; Sander, J.R.; Baltrusaitis, J.; Tivanski, A. V.; MacGillivray, L. R.; *J. Am. Chem. Soc.*, **2014**, *136*(19), 6778.
- Hoskins, B. F.; Robson, R.; *J. Am. Chem. Soc.*, **1990**, *112*, 1546.
- Fujita M.; Kwon, Y. J.; Washizu, S.; Ogura, K.; *J. Am. Chem. Soc.*, **1994**, *116*, 1151.
- Yaghi, O. M.; Li, G.; Li, H.; *Nature*, **1995**, *378*, 703.
- Gardner, D. G. B.; Lee, S.; Moore, J. S.; *J. Am. Chem. Soc.*, **1995**, *117*, 11600.
- Kondo, M.; Yoshitomi, T.; Seki, K.; Matsuzaka, H.; Kitagawa, S.; *Angew. Chem.*, **1997**, *109*, 1844. *Angew. Chem.* Int. Ed. Engl. **1997**, *36*, 1725.
- Schmidt, G. M. J. *J. Pure Appl. Chem.*, **1971**, *27*, 647 (b) Deshraj, G.R.; *Crystal Engineering: The Design of Organic Solids*; Elsevier : Amsterdam, **1989**.
- Nishio, M.; *Cryst. Eng. Comm.*, **2004**, *6*, 130.
- Desiraju, G. R.; *J. Mol. Struct.*, **2003**, *656*, 5.
- Moulton, B.; Zaworotko, M.; *J. Chem. Rev.*, **2001**, *101*, 1629.
- SAINT+, Bruker Analytical X-Ray Systems; *Madison, WI*, **2001**.
- Sheldrick, G. M. *SHELX-97*; Bruker Analytical X-Ray Systems; *Madison, WI*, **1997**
- Bala, S.; Bhattacharya, S.; Goswami, A.; Adhikary, A.; Konar, S.; Mandal, R.; *Cryst. Growth Des.*, **2014**, *14* (12), 6391.
- Viswamitra, M.A.; *J. Chem. Phys.*, **1962**, *37*, 1408.
- Jeffrey, G. A.; Parry, G. S.; *J. Chem. Soc.*, **1952**, *0*, 4864, DOI: 10.1039/JR9520004864.